The Impact of an Active Strike-slip Fault to The Principal Horizontal Stress Orientations and Fluid Flow in the Karaha Bodas Geothermal Field, Indonesia

Muhammad Ikhwan, R. Mochamad Tofan, Imam Muhammad Prasetyo, & Astha Dandari Kusuma Wardhani

Pertamina Geothermal Energy, Grha Pertamina, Jl. Medan Merdeka Timur, Gambir, Jakarta 10110

ikhwan.aziz@pertamina.com

Keywords: *Principal stress, geomechanics, structure, induced fracture, geothermal.*

ABSTRACT

The Karaha Bodas field is located in an active tectonic region which consists of complex volcano-stratigraphy and structural framework. To determine the best strategy for its development, we studied its tectonic setting and how it correlates with the productivity of a well using the geological evidence in a production well called WELL-A. The geological structure analysis from the image log data in WELL-A includes the identification of the maximum horizontal stress orientation along the well from the orientation of the drilling-induced fractures, including borehole breakout and drilling-induced tensile fractures or DITF. The maximum horizontal stress orientation is also determined from caliper data using the maximum and minimum size of the caliper to define the breakout or washout interval along the borehole. This image log analysis shows evidence of a rotation in the maximum horizontal stress in the reservoir rocks from N235°E to N200°E, which is strongly believed to be caused by the active NE-SW strike-slip Candramerta fault that was targeted by WELL-A. This active fault is also interpreted to contribute to production from the well as the response in the production log that is acquired in this well indicates a significant mass flow change at the fault. Overall, both the drilling-induced tensile fracture and caliper-breakout analysis capture the stress trend rotation and suggest the present-day principle horizontal stress orientation is directed NE to NNE. This is also similar to the regional stress data that suggest the maximum horizontal stress in West Java is oriented north-northeast.

1. INTRODUCTION

The Karaha-Bodas Geothermal Field is located to the north of G. Galunggung, about 20 km from Tasikmalaya in West Java, Indonesia. The Karaha Bodas Company (KBC) investigated the field, and drilled several exploration and full-size development wells, and later it was acquired by PT. Pertamina Geothermal Energy (PGE) who run a single flash plant with 30 MWe capacity operated at Karaha-Bodas. It is a complicated geothermal system because of its geological setting. The tectonic framework is believed to have evolved differently over time due to tectonic plate movement that dictates its geological structures. It has been subject to rapid magmatic intensity as the result of subduction between Indo-Australia and Eurasia tectonic plates that triggered the massive volcanic activities and added geological complexity. The relationship between this volcanic and tectonic activity has resulted in a unique geothermal system, characterized by the non-uniform geological structure, compartmentalized geothermal hydrology, and multiple types of permeability control that make the extraction of geothermal energy difficult.

Limited studies have characterized the tectonic activity related to the Karaha Bodas geothermal system and have successfully captured the geological structure of the Karaha Bodas field. Most of these works were produced by Nemcock et al. (2001 & 2004), and focused on the fracture studies from available well data including core and image logs. Moore et al. (2008) studied the evolution of the geothermal system in Karaha Bodas from the geochemistry and minerals analysis and deduced the fluid phase state that exists in the geothermal system.

All of these studies above were established during the exploration phase and used the early data in the Karaha Bodas field and need to be updated as the time gap between exploration and the current development stage is quite long. To date, more wells have been drilled to support electricity generation at Karaha Bodas and subsurface data has been acquired through the wells. This paper discusses the updated tectonic and kinematic study of the Karaha Bodas field based on the latest subsurface data. The study focuses on the geomechanics analysis through the image logs data and on how the new finding corresponds with the tectonic framework and its relationship with the productivity of the wells. This study focuses on the image log data acquired in WELL-A, located in the southern compartment of Karaha Bodas field and how the recorded data provides evidence of tectonic evolution from its attributes.

2. GEOLOGICAL OVERVIEW

Java Island is one of the volcanic islands of Indonesia that stretch from west to east consisting of Sumatra, Java, Bali, Lombok, Sumbawa and Flores, respectively. The existence of volcanism along these islands is directly related to the subduction of the Indo-Australian plate beneath the Eurasian plate which accommodates the relative northward movement of the Indo-Australian plate (Figure 1a). Hall (1997) has reconstructed the movement of the Eurasian tectonic plate in Southeast Asia and suggested that the plate has been stable for the last 10 Ma years. This information can be used to predict the tectonic and fracture kinematics of the present day and how they contribute to the hydrothermal fluid flow.

Java is located in a region with high seismic activity, known as the "Ring of Fire." It is home to numerous active volcanoes and experiences frequent earthquakes, due to its subduction. These geological processes can cause high levels of compression and tension, resulting in complex stress fields in the crust. Therefore, it is possible that Java Island is currently experiencing complex principal stresses due to the ongoing geological activity. However, the specific magnitudes and orientations of the stresses depend on a range of factors, such as the location and depth of the active geological features. The regional present-day principle stress from the World Stress Map database from USGS (2018) shows that the maximum horizontal stress in the West Java region is mostly directed to the NNE-SSW (Figure 1), as a result of the impact of Indo-Australia and Eurasia plates subduction. This tectonic setting influences the hydrology of the geothermal fluid in the Karaha Bodas field.

ISSN 2703-4275

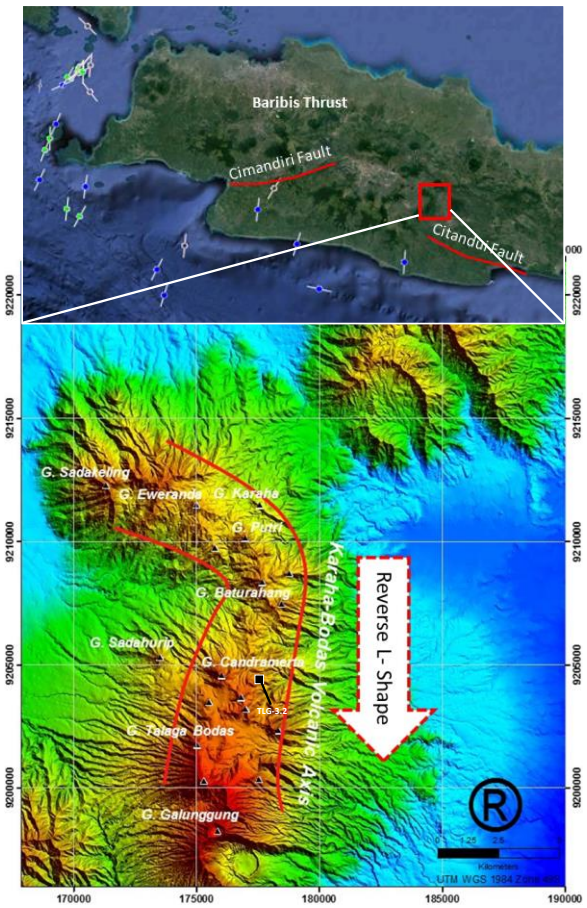

Figure 1: Upper) The tectonic and major structural framework of West Java and also the trend of maximum horizontal stress from World Stress Map data. Lower) The evolution of volcanic features in Karaha that relatively getting younger from north to south.

West Java is characterized by a diverse geological setting. The region is part of the Sunda Shelf, which is an extension of the continental shelf of Southeast Asia (Hall, 1997). The regional geology of West Java is primarily composed of volcanic rocks and sedimentary formations. The area is dominated by several volcanic complexes that are part of the Sunda Arc, a subduction zone that extends from Sumatra to Java. The volcanoes in West Java include Mount Salak, Mount Gede, Mount Pangrango, Mount Papandayan, and Mount Ciremai, and including Mount Galunggung near the Karaha Bodas field. These volcanic formations are characterized by stratovolcanoes, calderas, and lava domes. Sedimentary formations also play a significant role in the regional geology of West Java. These formations include sandstone, shale, limestone, and clay, which were deposited in ancient seas that covered the region during the Mesozoic and Cenozoic eras. The sedimentary rocks are found in several basins, including the Cimandiri, Bandung, and Sukabumi Basins. In addition to the volcanic and sedimentary formations, West Java also has several mineral deposits, including gold, copper, and coal. These resources are primarily found in the volcanic rocks of the region. To conclude, the regional geology of West Java is complex and diverse, with a combination of volcanic and sedimentary formations that have been shaped by tectonic processes and volcanic activity over millions of years.

The Karaha Bodas field is situated in the Bandung Central Volcanic Zone according to Van Bemmelen (1949). It consists of two major quaternary volcanic chains which are the Bandung Plateau which comprises Mt. Guntur and Mandalawangi, and the mountains in Citanduy and Cimanuk valley, including Mt. Galunggung, Talagabodas, Sadakeling, and Karaha (Figure 1c). The area is dominated by deposits from quaternary volcanoes with several volcanoes indicating the existence of thermal manifestations such as fumaroles and solfatara as post-volcanism products. Lava and andesite breccia are the majority of the rocks that overlie the area. Volcanic breccia and tuff were also deposited as a result of catastrophic collapse during the eruption of old Talaga Bodas Volcanic in the south. They could be acting as the reservoir rocks for the Karaha Bodas geothermal system.

The structural control in the field is also affected by the plate convergency as mentioned above. It occurs along the west–east trend, known as the Java structural trend. The Java trend is the youngest geological structure pattern cross-cutting the older Meratus (Late Cretaceous-Early Eocene) and Sunda (Early Eocene-Late Oligocene) trends that follow NE-SW and N-S directions, respectively (Simandjuntak and Barber, 1996). In the Western part of Java Island, the main structural geology trends are a) The back-arc thrust or Barabis-Kendeng thrust that crosscut the whole island along its northern part. Some segments of this thrust are still active, b) the NE-SW Cimandiri fault crosscuts from the southern coast to the northern coast, and c) the Citandui fault, that occurs in West Java with a WSE trend (Figure 11).

3. PREVIOUS STRUCTURAL STUDY

Previous fracture studies from Nemcok, et al. (2004) were conducted using data from 3 wells: corehole K-33, and two deep wells, KRH 2-1OH and KRH- 3-1ST. Data from the deep wells are based on the interpretation of electric image logs, while data from K-33 are based on detailed logging of the core. All these three wells are located in the northern part of the system near WELL-A and are separated by 5 km.

K-33 well was continuously cored from 754.3 to 2018.6 m with excellent recovery. Normal faults, tensile fractures, sinistral and dextral strike-slip faults, and sinistral and dextral oblique-slip faults with a normal component of displacement are present within the cap rock. They have been controlled by the strike-slip stress regime with horizontal maximum and minimum compressional principal stresses, σ1 and σ3, and vertical stress, σ2. Trends and plunges of principal stresses determined from well KRH 3-1ST, located just 3.4 km to the NW, are σ1 = 188/0, σ2=0/90 and σ3=98/0. Strike-slip regimes are missing in the reservoir. Instead, normal faults and tensile fractures are characteristic of the reservoir. They have been controlled by vertical σ1, and horizontal σ2 and σ3 principal stresses. Stress trends and plunges are: σ1=0/90, σ2=188/0 and σ3 98/0.

Well KRH 3-1ST is a deep full-sized exploration well. It has a total measured depth of 3078 m. An EMI log was obtained from 2117 m to 3016 m. The log shows that numerous normal faults/tensile fractures and dextral strike-slip faults have strikes of 350-30 dan 120-140, respectively. The less numerous sinistral oblique-slip, sinistral strike-slip and dextral oblique-slip faults strike 30-40, 50-70 and 140-170, respectively. There are few resistive fracture representations

ISSN 2703-4275

in well KRH -1ST. Electrically conductive fracture representations are dominant. Resistive fracture representations are always associated with non-producing fractures. Their resistive response in the image log is caused by resistive fracture fill, which is interpreted as calcite. The principle stress and fractured study from Nemcok (2004) in well KRH 3-1 ST determines the maximum horizontal stress orientation to be N188°E.

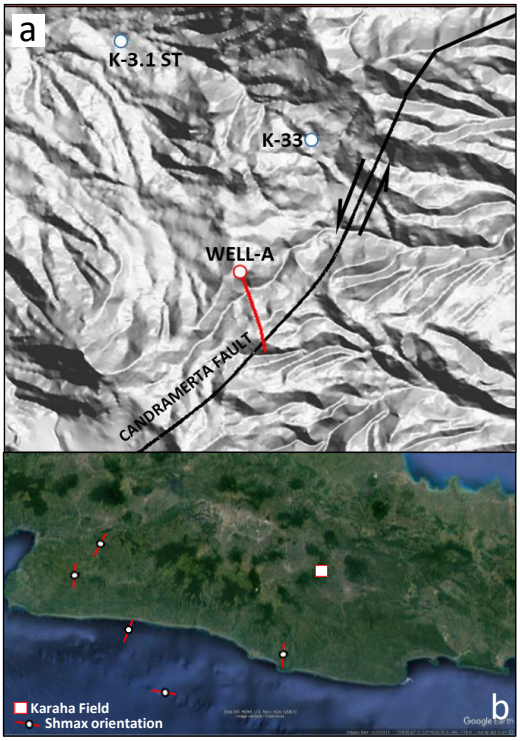

Figure 2: a) The orientation of WELL-A to the interpreted Candramerta fault as the target. Considering the fault has dip toward NE, the fault line represents the downside of the fault b) The regional orientation of maximum horizontal stress from World Stress Map data

Present-day horizontal geological stress orientation can be determined by measuring the strike of drilling-induced fractures (DITF) and also borehole breakouts in vertical or almost vertical wells. In deviated well they are more likely to represent the strain direction due to the stress applied on the wellbore (Zoback, 2007). However, previous stress analysis in deviated wells based on using DITF and breakout shows a good consistency and is an indicator of the actual principle horizontal stress. In simple terms, the DITF occur when the drilling pressure is much higher than the formation pressure while the borehole breakout happens when the drilling pressure is lower than the formation pressure. These features tend to be localized and track vertically down on opposing sides of the borehole. The strike orientation of borehole breakout provides the orientation of the minimum horizontal stress (Shmin) at the borehole wall, and the strike orientation of drilling-induced fractures indicate the maximum horizontal stress direction (Shmax). They are usually orthogonal to one another in the horizontal plane.

4. FOCAL MECHANISM SOLUTION

Focal mechanism solution (FMS) of microearthquake datasets detected by local seismic station networks during 2019-2022 were studied to get further understanding of structures and stress regime in Karaha. The strike azimuths of fault planes reveal various orientations, however, they are predominantly SW-NE and other possibilities being NNW-SSE & NNE-SSW. Some NE-SW and NW-SE fault trends are also observed. The orientations are somewhat in accordance with the regional maximum horizontal stress regional data and also mapped geological structure including the Candramerta fault. Using classification from Zoback (1992), the plunges of principal axis P and T from FMS were plotted to assign the stress regime as depicted in Figure 3. The P-axis often coincides with the axis of maximum compressional stress, while the T-axis is often equated with the axis of maximum tensional stress. However, the P and T axes actually indicate principal shortening and lengthening (strain) directions which may deviate significantly from the principal stress axes (Gephart, 1986). The results shows various stress regimes which might suggest that Karaha has a complex tectonics setting. However, the compressional stress regime including thrust and strike-slip faulting still dominates the plot which indicates the strong impact of southern subduction in Java.

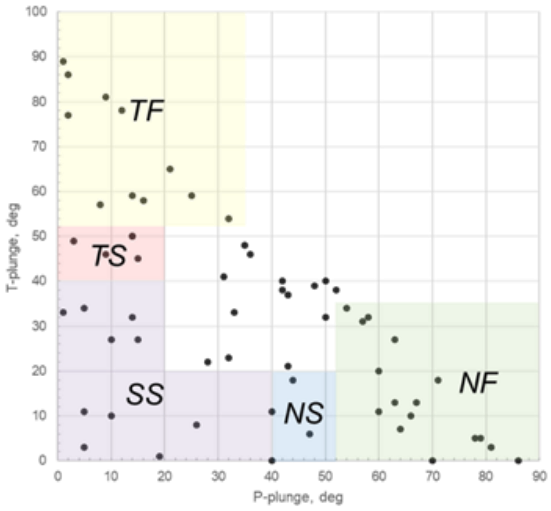

Figure 3: P- and T-plunge cross-plot from Karaha's FMS as tool to assign stress regime using classification from Zoback (1992). Black dots as focal mechanism solutions of microearthquakes, NF: normal faulting (shown as green zone); SS: strike-slip faulting (purple); TF: thrust faulting (yellow); NS: normal/strike faulting (blue); TS: thrust/strike faulting (pink). Stress regime of FMS outside the coloured zones is unknown.

5. BOREHOLE OBSERVATION

A number of wells were drilled in Karaha to support the 30 MW electricity production. WELL-A is located in the northern part of Mt. Talaga Bodas which is part of the southern compartment of Karaha field. It is directed to N260°E with total depth of 2500 mMD, targeting the Candramerta fault that is striking NE-SW (Figure 2a). This fault is partly represented on the surface topography and imagery and is interpreted as an older structure than the WNW-ESE faults which outcrop on the surface. With known fault and principal stress orientation, the kinematics and sense of movement of this fault are possible to predict. With NNE-striking maximum horizontal stress in the Karaha area

which forms ~35° angle to the NE-striking Candramerta fault plane, the Candramerta fault is interpreted as a left lateral strike-slip fault with minor normal slip.

A four-pad borehole image log tool (FMI) was acquired in WELL-A to characterize the subsurface geology in this area. FMI is a four-arm electrical imaging tool which can cover up to 75% of the borehole wall. FMI tools are also attached with a caliper pad that can measure the size and geometry of the borehole, and so the borehole breakout that disrupts the borehole size can also be detected. The log only measures the production interval or below the production casing shoe, starting from 1200 mMD to 2500 mMD. The result shows the subsurface lithology mostly dominated by pyroclastic, including tuff and volcanic breccia, and lava. The source of these volcanic products is believed to be derived from multiple volcanic eruptions and different events as WELL-A situated in the Candramerta crater and several volcanic bodies appear in the vicinity. However, no sedimentary formation was intersected, which confirms the intensive volcanic events in the Karaha Bodas field that overlays the area with a thick volcanic product. The image log consists of intense fractures, including conductive fractures, resistive fractures, joint, bed boundary, borehole breakout, and drilling-induced tensile fractures (DITF). Medium and strong washouts are presented in the image, nevertheless, it is still unclear whether they are caused by the mechanical properties or unconsolidated formations. The natural fractures from WELL-A consistently show the NNE to NE orientation, varying from N35°E ±10° and agree with the orientation of the Candramerta fault as the main target of the well.

5.1 Fractures analysis

There are several fracture type that can be identified from the image log data including the conductive and resistive fractures. The open and permeable fracture might be associated with the conductive fracture deduced from the image log interpretation. Yet, it is important to note that the conductive fracture with a dark appearance on the image log could be interpreted in two ways: open fracture or mineral-filled fracture such as clay. The fracture stability analysis examines the critically stressed fracture, which is interpreted as the permeable fracture or possibly open fracture, by measuring its slip tendency ratio (Barton et al., 1995). Once a stress regime is identified, normal and shear stresses on fractures orientation available in image log data can be determined, and their slip tendency can be calculated (Townend & Zoback, 2000).

Fractures with high slip tendency are at an orientation (strike and dip) where they are more likely to experience shear failure given the magnitude and orientation of the effective stress tensor, where the effective stress tensor is the maximum σ1, intermediate σ2, and minimum σ3 tectonic stresses minus the oppositional force of pore fluid pressure. We use these conductive fractures data, such as strike and dip, rotating them into the geographical coordinate by using the method from Zoback (2007), to cluster which of those fractures are critically stressed (Figure 4). Barton et al. (1995) suggest that normally the possible stressed open fracture would have the shear stress to the normal stress ratio between μ = 0.6 and μ = 1.0. This analysis gives the trend of fractures that could possibly contribute to the fluid flow.

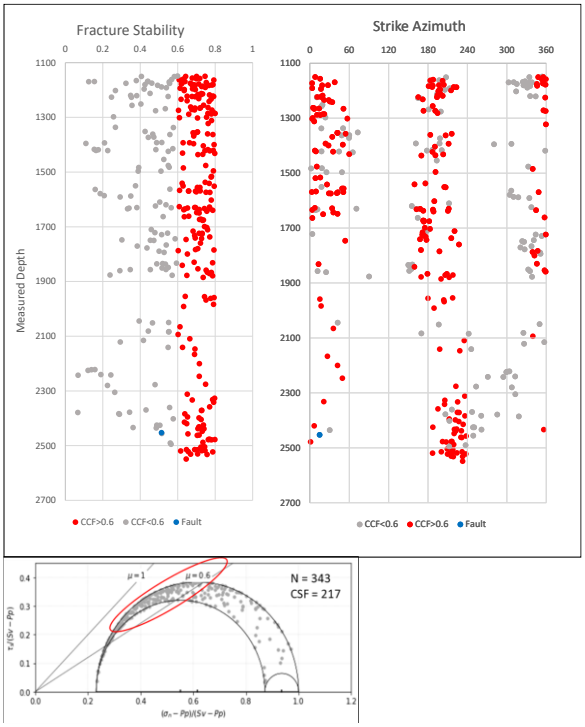

Figure 4: Fracture stability analysis for the conductive fractures in the Well-A. Red dot indicates the critically stressed fracture that possibly open. Red circle in Mohr Coloumb indicates the fractures that have μ > 0.6 or above the failure envelope line

Well-A has a high fracture intensity, including conductive fractures. This high-intensity fracture zone might still relate to the well direction that is perpendicular to the Candramerta fault and also the maximum horizontal stress direction. These fractures are distributed along the production zone interval or in the open-hole trajectory. A total of 343 conductive fractures were identified in this well. From the geomechanics analysis, more than half of these conductive fractures are critically stressed fractures with a dominant NNE-SSW orientation. The fracture and fault data in three-dimensional Mohr representations (shear vs effective normal stress normalized by the vertical stress) are shown in Figure 3. As indicated by the Coulomb failure lines μ = 0.6 and μ = 1.0, most of the conductive fractures in Well-A appear to be critically stressed on the strike-slip fault regime model with the maximum horizontal stress oriented to N25°E, which indicates potentially active faults in frictional equilibrium with the in-situ stress field. This finding increases the confidence level to assume the hydrology of the reservoir fluid is trending north-northeast.

5.2 Borehole induced-fractures

Borehole fractures are the result of a severe difference in the pressure of the drilling mud introduced into a bore and the hydrostatic pressure of the material through which the bore is drilled. Drilling-induced tensile fractures (DITF) are the most common and easily visible induced fractures observed in image logs and core. Distinguishing between induced fractures and natural fractures in core samples or image logs involves a visual assessment of the surface characteristics of the fractures and the spatial arrangement between the core and fracture patterns, including the starting flaw and the path

ISSN 2703-4275

of propagation. It is not possible to definitively determine whether an individual fracture is natural or induced solely based on its trace in an image log. However, when considering a group of fractures, their origin can be deduced from image log data due to the distinct geometries of natural and induced fractures in the wellbore. If breakouts are present and the stress field in which the natural fractures formed differs significantly from the current stress conditions, then the orientation of the fractures relative to the breakouts can serve as an additional (though less precise) criterion for distinguishing between these two types of fractures (Lacazette et al., 2013). Borehole breakouts form as the result of compressive failure, which causes the caving in of the borehole wall. For breakouts to form, the circumferential stress at the borehole wall must exceed the compressive strength of the rock. Fractures are commonly caused by stress exceeding the strength of the rock, causing the rock to lose cohesion along its weakest plane. Fractures can provide permeability for fluid movement, such as water or hydrocarbons.

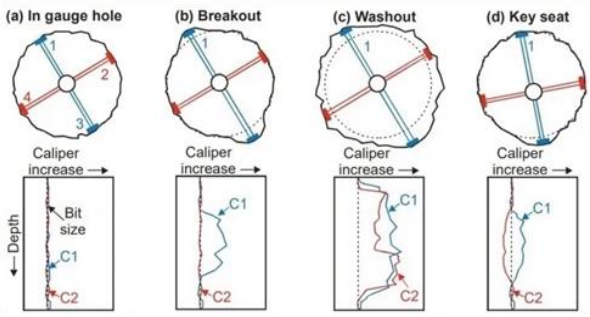

Figure 5: Common types of enlarged borehole and their caliper log response (Heidbach et., 2016)

5.3 Drilling-induced Tensile Fracture (DITF) Analysis

In Well-A, DITF dominates the drilling-induced fractures, remarks the downhole pressure was often greater than the formation pressure (Figure 6). Along the 1300 open hole section, many DITF were measured in the WELL-A. The DITF occurrence intensity can be separated into two groups based on their interval; i) Group I, 77 DITF in this group are accumulated between 1200 to 1950 mMD and on average strike to N235°E, ii) Group II, 384 DITF recognized along 1950 to 2500 mMD which mostly directed to N200°E. The boundary depth between these two groups also coincidentally aligns with the borehole size change between the 12 1/4" hole and 9 7/8" hole. There are significant DITF counts from these two groups, where the DITF in Group I is fewer than that in Group II. Despite the mechanical properties of the drilling parameter applied during drilling to the borehole formations, this phenomenon could also have been caused by the dominant lithology present in the borehole. The 12 1/4" hole dominantly consist of andesitic lava, which might have higher compressional strength than the pyroclastic breccia that dominate the 9 7/8" inch hole. However, further identification of the applied drilling mud pressure and geomechanics analysis are needed to confirm the reason for the DITF intensity gap.

Another distinguished stress characteristic recorded from the DITF is the occurrence of maximum horizontal stress counterclockwise significant rotation. The Group I DITF is oriented to N235°E while Group II is oriented slightly more NNE-SSW / N200°E which shows a ±30° difference. This exactly occurs somewhere between 1950 mMD to 2030 mMD, or on the interval where the image log does not cover the borehole wall because the hole size transitions between 12 1/4" hole and 9 7/8" hole. The stress perturbation might be caused by many factors, including the occurrence of a fault, fractures or lithological contact (Lin et al., 2010). However, as WELL-A targets the NE-striking Candramerta fault with a sense of left lateral strike-slip, the stress rotation is strongly interpreted as being triggered by the occurrence of such fault. The presence of the associated strike-slip fault or fractures at the stress rotation depth is unidentified as the image log is absent at such intervals.

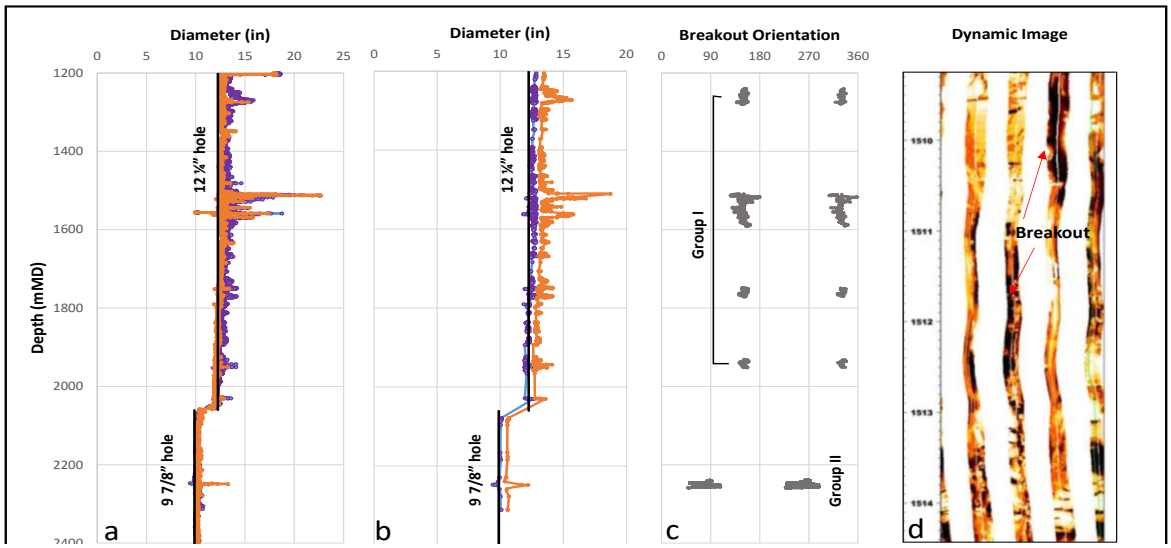

Figure 5. a) The raw plot of caliper data (minimum and maximum caliper) in 12 ¼" and 9 7/8" hole. b) Selected FMI caliper data meeting the three quality criteria given in the text. c) Selected borehole breakout orientation from caliper size analysis. d) Example of a large washout due to breakout recorded in image log at 1510 and 1512 mMD that makes the calipers slightly rotated and disoriented. The breakout features are also hindered by the limited pads coverage.

5.4 Borehole-breakout Analysis

The stress orientation is also possibly identified from the borehole breakout, as it represents the minimum horizontal stress direction. Nonetheless, some breakouts cause the borehole washout that is captured on the image log and disrupt the breakout appearance. Fewer appearances of breakout could also be the consequence of the homogeneity of the stress ratio magnitude in formation. In principle, a breakout occurs once the circumferential stress s_c at the borehole wall in the minimum stress azimuth exceeds the compressive strength of the rock. This stress s_c is expressed as $s_c = 3S_{Hmax} - S_{hmin} - P_p - P_m$, where P_p and P_m are pore pressure and mud pressure, respectively (Zoback, 2007), so s_c is mostly controlled by the S_{Hmax}. These observations indicate that the S_{Hmax} magnitude profile may be a simple direct proportion relationship with depth. Fortunately, the caliper data can be used to predict the presence of borehole breakout. The breakout potentially enlarges the borehole diameter size which can be detected from the caliper tool. The inclinometer attached to the caliper pad can measure the enlargement or elongation orientation due to breakout. The details of the method are discussed below.

The borehole breakout occurs when the formation pressure is much higher than the drilling pressure. As the pressure issue is normally not important in geothermal wells, borehole breakouts tend to be fewer or absent, especially for a well that is not indicating geomechanical concerns in the drilling parameter, for instance, the safe mud weight window calculation. However, the absence of borehole breakout in the image log could also be caused by the image coverage that coincidently might not be covered by the image log pads. Therefore, this study attempts to identify the borehole breakout in the well from the raw caliper data available, as proposed by Lin et al. (2021) (Figure 5a). When detecting breakouts from the data obtained by the four-arm caliper, we applied three quality control criteria similar to those outlined by Plumb (1985). Initially, the disparity between the larger caliper diameter (C1) and the smaller diameter (C2) should be substantial, being at least 0.05 times the diameter of the drill hole (D). Additionally, the smaller caliper diameter should remain within 1.05 times the drilling diameter (D). Lastly, both caliper diameters should not deviate significantly from the bit diameter, meaning that both C1 and C2 should be greater than 0.95 times the drilling diameter (D). This generated a subset of the caliper data for predicting the occurrence of borehole breakout (Figure 4b) which displays the breakout elongation and also the gaps between the minimum and maximum calipers log especially in the 12 ¼" hole around 1273 mMD, 1510 mMD, 1562 mMD, 1935, and 1770 mMD, and also washout in the 9 7/8" hole around 2248 mMD (Figure 4c,d). There are more appearances of breakout in the 12 ¼" hole than the 9 7/8" hole indicating the downhole pressure in the 9 7/8" inch hole was much higher than the formation pressure which is also indicated by the significant intensity of DITF.

As all indicated breakouts from the caliper analysis has been identified, we estimated the S_{Hmax} orientation by add the 90° to the breakout angle azimuth whereas the breakout is representing the minimum S_{hmin} and the S_{Hmax} is always perpendicular to the S_{hmin}. The orientation of maximum horizontal stress analysis from the breakout angle can also be grouped according to the DITF analysis in which a breakout in Group I is higher than in Group II. The average S_{Hmax} orientation from a breakout in group I is N239°E with a deviation of ±6° while the average S_{Hmax} orientation from a breakout in group II is N353°E with a deviation of ±15°. It is also indicating the maximum horizontal stress orientation between group I and II. However, as the image log interprets the borehole elongation in group II as a washout that could

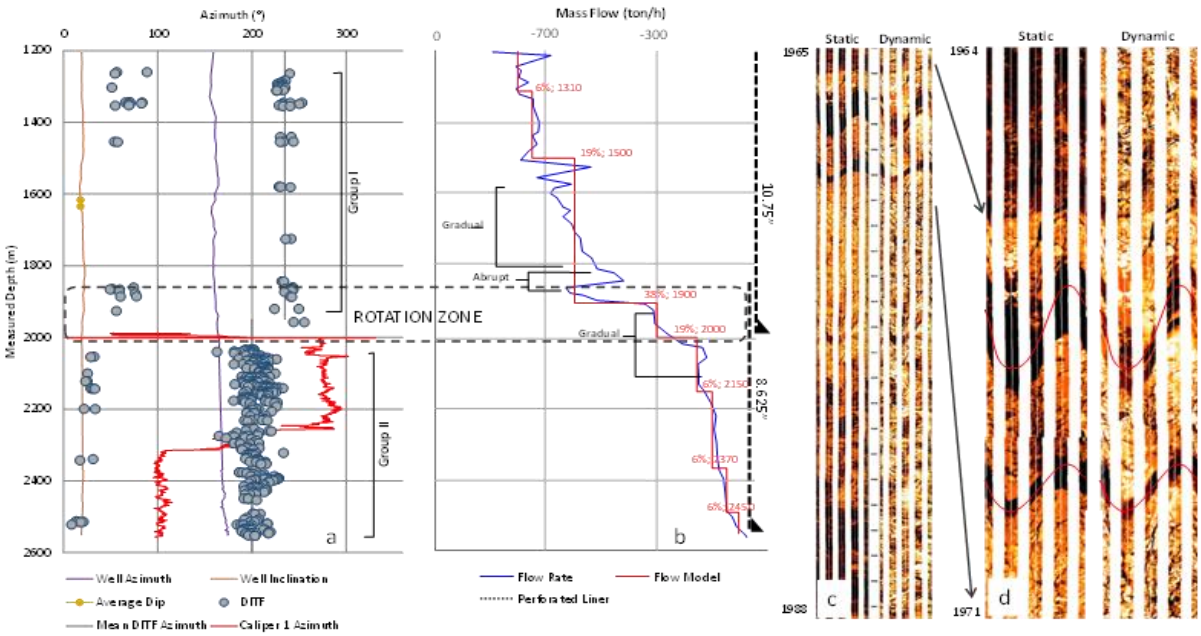

Figure 6. a) The distribution of DITF along the production interval in WELL-A. The stress rotation zone detected between the 12 ¼" hole and 9 7/8' hole and this interval also contributes to the well's productivity (feedzone). This zone corresponds with the significant flow from the spinner data (b) which indicates 38% and 19% mass flow change. c) and d) shows the evidence of the north-northeast fractures with a wide aperture on the image log (red sinusoids).

ISSN 2703-4275

also be influenced by a formation collapse or fault. The maximum horizontal stress orientation in the 9 7/8" hole is more prominent as confirmed by the DITF that abundantly occur.

6. STRESS ROTATION CONTRIBUTION

WELL-A is a production well. The production log test or spinner test during injection was run to investigate the production interval by identifying changes in the flow model graph caused by changes in spinner velocity in the permeable zones or feedzones. Several productive intervals are determined and two of them are located on the interval where the DITF orientation rotates due to a particular reason (Figure 6). As this interval contributes significantly to the mass flow change, we interpret that the rotation in DITF orientation could be caused by an active strike-slip fault, as targeted by WELL-A. The evidence of intersected fracture or fault zone with wide fracture aperture is shown by the image log on interval 1964 mMD to 1971 mMD. There are two continuous conductive fractures recorded on the image log, one of them has an aperture of approximately 1 meter. The conductive (dark features) fractures might be filled by fluid. Therefore, these fractures or fault zone were interpreted as a part of the active Candramerta fault zone and contributes to the significant flow in this interval that was proved by spinner logging tools. The existence of a faults zone is also indicated by the type of mass flow change in the spinner response. The shape of the mass flow change graph can determine the permeability control type. An abrupt flow change mostly indicates a highly permeable feature, such as a wide aperture fracture or a lithological contact, while the gradual change might be caused by a high-intensity fracture zone or a permeable unit.

In addition, an active fault has a good opportunity to become a conduit to the hydrothermal fluid as it could maintain the fractures aperture and also prevent the secondary mineral depositions that could reduce the permeability if they are not actively removed by the moving fault.

7. CONCLUSION & DISCUSSION

Karaha Bodas geothermal field is showing different structural frameworks between surface and subsurface structural configurations. As the reservoir is buried at depth, the identification of its structural framework becomes critical to understanding the potential fluid flow behaviour and in identifying future well targets. The Karaha field is dominated by surface NW-SE structural lineaments yet WELL-A is targeted at the NE-SE Candramerta fault. This target fault is well-interpreted from the borehole data including the image log. This fault also influences the tectonic setting including the local horizontal stress in depth. Analysis of horizontal stress orientation was conducted from the induced-fracture appearance in the image log, including the DITF and borehole breakout. The induce-fractures in WELL-A can be grouped into two; group I and group II which differ in the intensity of the fracture. Both of these induced fractures agree with the idea that the orientation of maximum horizontal stress in Karaha is mostly oriented to NE-SW. This horizontal stress orientation is also similar to the regional stress orientation shown by the World Stress Map data. WELL-A also encountered the stress rotation zone, which was shown by the ±30° changes of the maximum horizontal stress orientation from the 12 ¼" hole to the 9 7/8' hole. This stress orientation is strongly influenced by the Candramerta fault, which is interpreted as an active left-lateral strike-slip fault and has a sufficient fluid flow contribution to the well.

The results of the tectonic framework study of Karaha can strongly support the future well-targeting and field development strategy. Mechanically, an active fault can be a good target for a geothermal well as it is potentially permeable for the hydrothermal fluid flow. The stress analysis from the WELL-A image log reveals the NE-SW structure and its associate fractures, or the structure that likely parallels the maximum horizontal stress orientation, like the Candramerta fault, and suggest it is reasonably promising as a well target. The challenge in this field is that these structures are mostly doubly exposed on the surface and that means the structural framework at depth is uncertain. In this case, the geological concepts and the supporting geophysical data can be used to strengthen the subsurface geological interpretation and imaging to determine the reservoir configuration.

ACKNOWLEDGEMENTS

We acknowledge PT. Pertamina Geothermal Energy provided data and permission to publish this paper. We thanks Irene Wallis for providing the Python code for the 3D Mohr plot and geomechanics modelling.

REFERENCES

Barton, C. A., Zoback, M. D., and Moos, D.: Fluid flow along potentially active faults in crystalline rock: Geology, v. 23, p. 683-686. (1995)

Gephart, J.W.: Principal Stress Directions and The Ambiguity in Fault Plane Identification From Focal Mechanisms: Bulletin of The Seismological Society of America, Vol 78, (1986), 621-625.

Hall, R : Cenozoic plate tectonic reconstructions of SE Asia. Journal of Asian Earth Sciences 20(4):353-431F.DOI: 10.1016/S1367-9120(01)00069-4 (1997)

Heidbach, O., M. Rajabi, X. Cui, K. Fuchs, B. Müller, J. Reinecker, K. Reiter, M. Tingay, F. Wenzel, F. Xie, M. O. Ziegler, M.-L. Zoback, and M. D. Zoback : The World Stress Map database release 2016: Crustal stress pattern across scales. Tectonophysics, 744,484-498. http://doi.org/10.1016/j.tecto.2018.07.007 (2018)

Lacazette, Alfred & Vermilye, Jan & Sicking, Charles & Geiser, Peter : Direct Imaging of Natural Fracture Flow Networks at the Reservoir Scale. 2nd EAGE Workshop Naturally Fractured Reservoirs: 10.3997/2214-4609.20132019 (2013)

Lin, W., En-Chao Yeh, Jih-Hao Hung, Bezalel Haimson, Tetsuro Hirono : Localized rotation of principal stress around faults and fractures determined from borehole breakouts in hole B of the Taiwan Chelungpu-fault Drilling Project (TCDP), Tectonophysics, Volume 482, Issues 1–4, (2010)

Lin, Weiren & Doan, Mai-Linh & Moore, J. & Mcneill, Lisa & Byrne, Timothy & Ito, Takatoshi & Saffer, D.M. & Conin, Marianne & Kinoshita, Masataka & Sanada, Yoshinori & Thu, Moe & Araki, Eiichiro & Tobin, Harold & Boutt, David & Kano, Yasuyuki & Hayman, Nicholas & Flemings, Peter & Huftile, Gary & Cukur, Deniz & Kido, Yukari : Present-day principal

horizontal stress orientations in the Kumano forearc basin of the southwest Japan subduction zone determined from IODP NanTroSEIZE drilling Site C0009. Geophysical Research Letters. 37. L13303. 10.1029/2010GL043158 (2021)

Nemcock, M., McCulloh, J, Nash, G., & Moore, J : Fault kinematics in The Karah-Talaga Bodas, Indonesia, Geothermal Field: An Interpretation Tool for Remote Sensing Data. Geothermal Resources Council Transactions, Vol.25 Augustus (2001)

Nemcock, M., Moore, J., Allis, R., & McCulloh, J : Fracture development within a stratovolcano: the Karaha-Telaga Bodas geothermal field, Java volcanic arc. Geological Society, London, Special Publications, 231, 223-242 (2004)

.Moore, J., Allis, R., Nemcock, M., Powell, T., Bruton, C., Wannamaker, P., Raharjo, I. B., & Norman, D : The Evolution of Volcano-Hosted Geothermal Systems Based on Deep Wells from Karaha-Telaga Bodas, Indonesia. American Journal of Science, Vol. 308, January, P. 1–48, DOI 10.2475/01.2008.01 (2008)

Plumb, R. A : Stress induced borehole elongation: comparison 769 between the four-arm dip meter and the borehole televiewer in the Auburn 770 geothermal well, J. Geophys. Res., 90, 5513–5521, doi:10.1029/JB090iB07p05513 (1985)

Towned, J., & Zoback, M, D.: How faulting keeps the crust strong. Geology. https://doi.org/10.1130/0091-7613(2000)28<399:hfktcs>2.0.co;2. (2000)

van Bemmelen RW : The Geology of Indonesia, vol. I a:general geology. Nijhoff, The Hague, 732 pp (1949)

Zoback, M. : Reservoir Geomechanics. Cambridge: Cambridge University Press. doi:10.1017/CBO9780511586477 (2007)

Zoback, M.L., 1992. First- and second-order patterns of stress in the lithosphere: The World Stress Map project. J. Geophys. Res., 97, 11,703-11,728.

ISSN 2703-4275